

UC Irvine

UC Irvine Previously Published Works

Title

Design limitations of a photoacoustic probe for port wine stain depth determination

Permalink

<https://escholarship.org/uc/item/1t9099pf>

Authors

Viator, John A
Au, Gigi
Choi, Bernard
[et al.](#)

Publication Date

2002-06-10

DOI

10.1117/12.469861

Copyright Information

This work is made available under the terms of a Creative Commons Attribution License, available at <https://creativecommons.org/licenses/by/4.0/>

Peer reviewed

Design limitations of a photoacoustic probe for port wine stain depth determination

John A. Viator^a, Gigi Au^b, Bernard Choi^a, and J. Stuart Nelson^a

^aBeckman Laser Institute, University of California, Irvine, CA, USA

^bHarvey Mudd College, Claremont, CA

ABSTRACT

We designed a photoacoustic probe to determine the depths of epidermal melanin layer and port wine stain (PWS) in human skin. We present experimental data showing limitations in its use. We developed acrylamide tissue phantoms with optical properties matched to those of human PWS skin. We determined the limit in resolving epidermal and PWS layers. Additionally, we determined the maximum epidermal melanin concentration that allowed threshold detection of the PWS layer. Finally, we compared the photoacoustic signals from the tissue phantoms and human PWS skin.

Keywords: optoacoustic, PVDF, acoustic transducer, Q-switched, acrylamide, optical fiber, skin

1. INTRODUCTION

Laser treatment of port wine stains (PWS) uses a pulsed laser to cause thermal damage to ectatic blood vessels which compose the lesion. Such damage is caused by selective absorption of laser energy by blood within the vessels. However, epidermal melanin, a broadband optical absorber, decreases laser fluence at the PWS. Additionally, for skin with a relatively high content of melanin (usually skin types III or higher [1]), the temperature of the epidermis may rise to an unacceptably high level resulting in damage and possibly permanent scarring of the skin surface. As a remedy, clinicians have instituted epidermal cooling, such as dynamic cryogen spray cooling (CSC) [2, 3]. While the superficial melanin cools nearly instantaneously, the resultant cold front will not reach the deeper PWS until some later time, preferably long after the therapeutic laser pulse has elevated the temperature of the PWS. Knowing the actual depth of the PWS would allow the clinician to optimize CSC parameters without cooling the PWS. Thus, we have developed a photoacoustic probe for determining PWS and epidermal melanin depth quickly and noninvasively.

The use of photoacoustic phenomena is ideally suited for the application of determining skin structure due to the high resolution and robust acoustic signal. Hence, analysis of photoacoustic waves has been used to investigate layered structures in tissue and tissue-like media. Oraevsky *et al.* [4] derived optical properties of absorbing solutions by fitting the photoacoustic signal to Beer's law. Viator *et al.* [5] derived an iterative scheme for determining the absorption coefficient of layered gels and stained elastin from the photoacoustic waves. Viator *et al.* developed an endoscopic photoacoustic probe for determination of treatment depth after photodynamic therapy for esophageal cancer [6]. Previously, we developed a probe to determine the epidermal and port wine stain (PWS) depths in human subjects using a photoacoustic reflectance probe [7]. We present an evaluation of the probe, specifically to determine the limitations of its use in human patients.

In planar layered media, we model photoacoustic propagation as plane waves, according to the equation,

$$p(z) = \frac{1}{2} \Gamma H_0 \mu_a e^{(\mu_a z)} \quad (1)$$

which predicted the photoacoustic pressure (J/cm^3). Viscoelastic attenuation was neglected in this analysis. The factor of $\frac{1}{2}$ accounted for the bi-directional generation of the acoustic wave, meaning that half of the

Further author information: (Send correspondence to J.A.V.)

J.A.V.: E-mail: javiator@laser.bli.uci.edu, Telephone: 1 949 824 3754,

Address: 1002 Health Sciences Road East, Irvine, CA 92612, USA

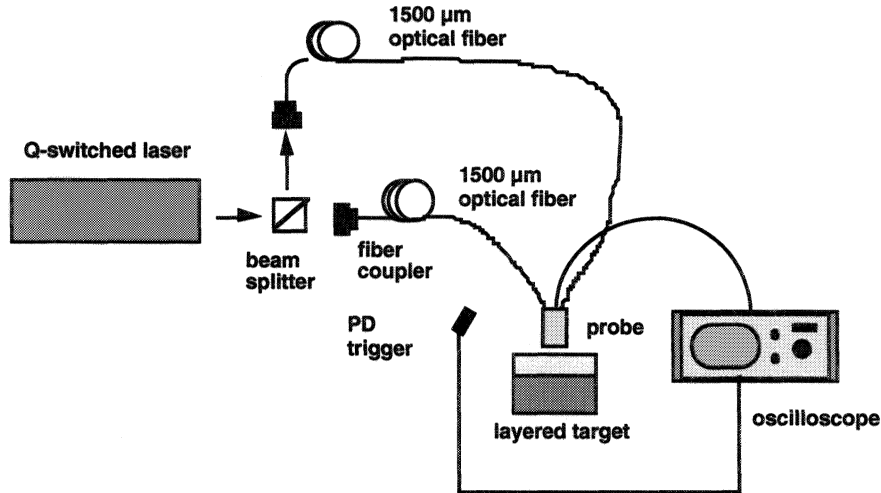


Figure 1: The experimental apparatus for the photoacoustic experiments.

acoustic energy traveled toward the detector immediately, while the other half traveled away. Γ is the Grüneisen coefficient, which models the fraction of optical energy converted to acoustic energy. In this analysis, $\Gamma = 0.12$ was used [4], [8]. H_0 is the radiant exposure (J/cm^2), and μ_a is the absorption coefficient of the solution in cm^{-1} . Finally, the conversion $10 \text{ bar} = 1 \text{ J}/\text{cm}^3$, was used to determine a calibration factor of mV/bar for the acoustic detector by dividing the amplitude of the acoustic waveform by the calculated pressure. Thus, the absorption coefficient, μ_a , can be determined by the plane wave shape or the amplitude. For PWS depth, we use the product of the wave speed, c_s , equal to $1.5 \text{ mm}/\mu\text{s}$, and the acoustic propagation time.

2. MATERIALS AND METHODS

We determined the limitations of the photoacoustic probe by finding the limit of resolving two absorbing layers separated by a clear layer. Additionally, we determined the highest epidermal melanin concentration that would allow generation of a detectable photoacoustic signal from a PWS layer. This determination was done experimentally with tissue phantoms and verified using plane wave analysis of equation 1.

2.1. Apparatus

The experimental apparatus is shown in figure 1. It consisted of a frequency-doubled, Nd:YAG laser operating at 532 nm with a 5 ns pulse duration. The laser light was launched into two $1500 \mu\text{m}$ optical fibers via a cube beamsplitter. Two fibers were used to increase the total amount of energy delivered while keeping patient discomfort to a minimum. The fibers terminated in the photoacoustic probe. The acoustic transducer element within the probe sent a signal via a 10Ω coaxial cable to an oscilloscope (Tektronix TDS 3014, Wilsonville, OR) with a bandwidth of 100 MHz . The input impedance of the oscilloscope was $1 \text{ M}\Omega$. The output energy of each fiber was approximately 11 mJ . The optical fibers were steered via set screws within the acrylic handpiece so that both laser spots were coincident. The probe was placed in contact with tissue phantoms so that the photoacoustic waves were generated directly below the acoustic detector. Subsequent photoacoustic analysis was done on a computer.

2.2. Probe Design

The probe design was fully described in Viator *et al.* [7]. It is shown pictorially in figure 2. A photograph of the probe is shown in figure 3. It consisted of two $1500 \mu\text{m}$ optical fibers terminating into a cylindrical acrylic handpiece 22 mm long and 16 mm in diameter. The laser spot was slightly elliptical with a diameter of approximately 2 mm . The radiant exposure at the surface of the phantoms was $0.70 \text{ J}/\text{cm}^2$. A semi-rigid

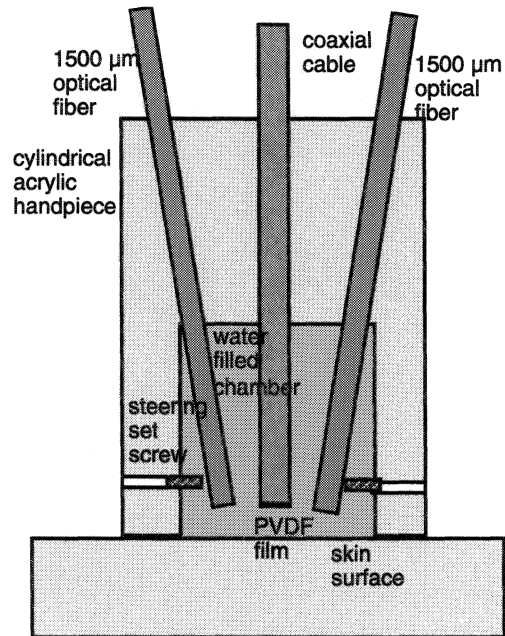


Figure 2. The photoacoustic probe consisted of two 1500 μm optical fibers and a PVDF sensing element. The output ends of the fibers and the PVDF were set within a chamber which was filled with water for acoustic coupling for the target surface. Set screws were used to steer the fiber ends to direct the laser spot directly beneath the PVDF.

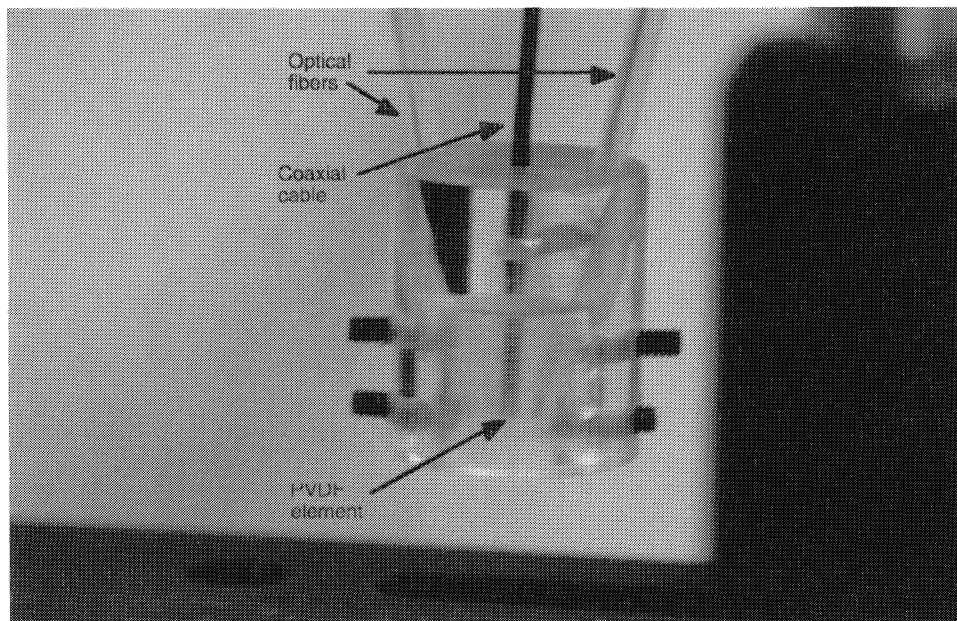


Figure 3. The actual probe is shown here. The rigid coaxial cable is clearly seen extending into the inner chamber of the probe.

Table 1. Optical properties used for the experiments for determining the maximum epidermal melanin content for threshold detection of a photoacoustic PWS signal.

Layer	Thickness (μm)	μ_a (cm^{-1})	μ_s (cm^{-1})	Optical depth
epidermis	75	8,20,52, 80	200	0.08, 0.15, 0.34, 0.5
dermis	250	0.2	200	0.03
PWS	1000	25	200	2.5

coaxial cable (UT-43-10, Micro-Coax, Pottstown, PA) with a diameter of 1.1 mm was inserted into the probe with a piezoelectric film attached to the end. The film was a polyvinylidene fluoride film (PVDF) (K-Tech, Albuquerque, NM). The active area of the acoustic sensor was $700\ \mu\text{m}$ in diameter. Thus, the optical fibers irradiated the tissue surface, inducing photoacoustic waves, which were sensed in reflection mode by the PVDF sensor. The fibers and the sensor were housed in a water filled chamber, which allowed for acoustic impedance matching between the tissue surface and the sensor. The signal was transmitted via the coaxial cable to an oscilloscope.

2.3. Layered Acrylamide Phantoms

Tissue phantoms were made with 20% acrylamide in water with added dye for absorption and fat emulsion for scattering. The amount of dye and fat emulsion were chosen to mimic the optical properties of human skin. Direct Red 81 (Sigma Chemical, St. Louis, MO) was used to simulate hemoglobin absorption and Intralipid (Abbot Laboratories, North Chicago, IL) was used to induce light scattering. A 1% Intralipid solution was used to approximate $200\ \text{cm}^{-1}$, the scattering coefficient of human skin [9–11]. Effective attenuation, μ_{eff} , was calculated using the value of 0.9. The procedure for preparing the acrylamide is fully discussed in [7].

Two types of phantoms were prepared. Both were three layered, representing epidermis, normal dermis, and PWS. Acrylamide solutions were injected between glass slides with plastic feeler gauge stock of various thickness used as spacers (Feeler gauge stock, McMaster-Carr, Los Angeles, CA). In the first set of experiments, the minimum distance that the probe could discriminate between the two absorbing layers (epidermis and PWS) was studied. These epidermal and PWS layers were purely absorbing, with absorption coefficients of $25\ \text{cm}^{-1}$, and the normal dermis layer was clear. In the second set of experiments, the phantoms were turbid. These experiments were meant to determine the maximum epidermal melanin concentration that would allow detection of a photoacoustic signal from the PWS layer.

2.3.1. Layer Discrimination

The epidermal layers were $100\ \mu\text{m}$ thick, while the PWS layers were approximately 1 mm thick. The clear layers were 70, 140, 350, 450, 770, and $1030\ \mu\text{m}$ thick. The three layers were placed on top of each other. Enough moisture was present to ensure acoustic coupling. Any air pockets between layers was removed. After laser irradiation, the layers were measured with a micrometer with a resolution and accuracy of $1\ \mu\text{m}$ (Mitutoyo micrometer, McMaster-Carr, Los Angeles, CA).

2.3.2. Epidermal Melanin Filtering

To model skin with various epidermal melanin content, we used turbid phantom layers with a scattering coefficient of approximately $200\ \text{cm}^{-1}$ [9]. The optical absorption was varied to model 2, 5, 13, and 20% epidermal melanin volume fraction [1]. We assumed a melanin absorption coefficient of $400\ \text{cm}^{-1}$ at 532 nm. The optical depths corresponded to 0.06, 0.15, 0.39, and 0.60, as the layer thickness was $75\ \mu\text{m}$. The optical properties and layer thicknesses of the phantoms are explicitly shown in table 1.

3. RESULTS

3.1. Layer Discrimination

A montage of photoacoustic waves is shown in figure 4. They represent laser irradiation of three layered phantoms with clear layer separations of 70, 140, 350, 450, 770, and $1030\ \mu\text{m}$ each.

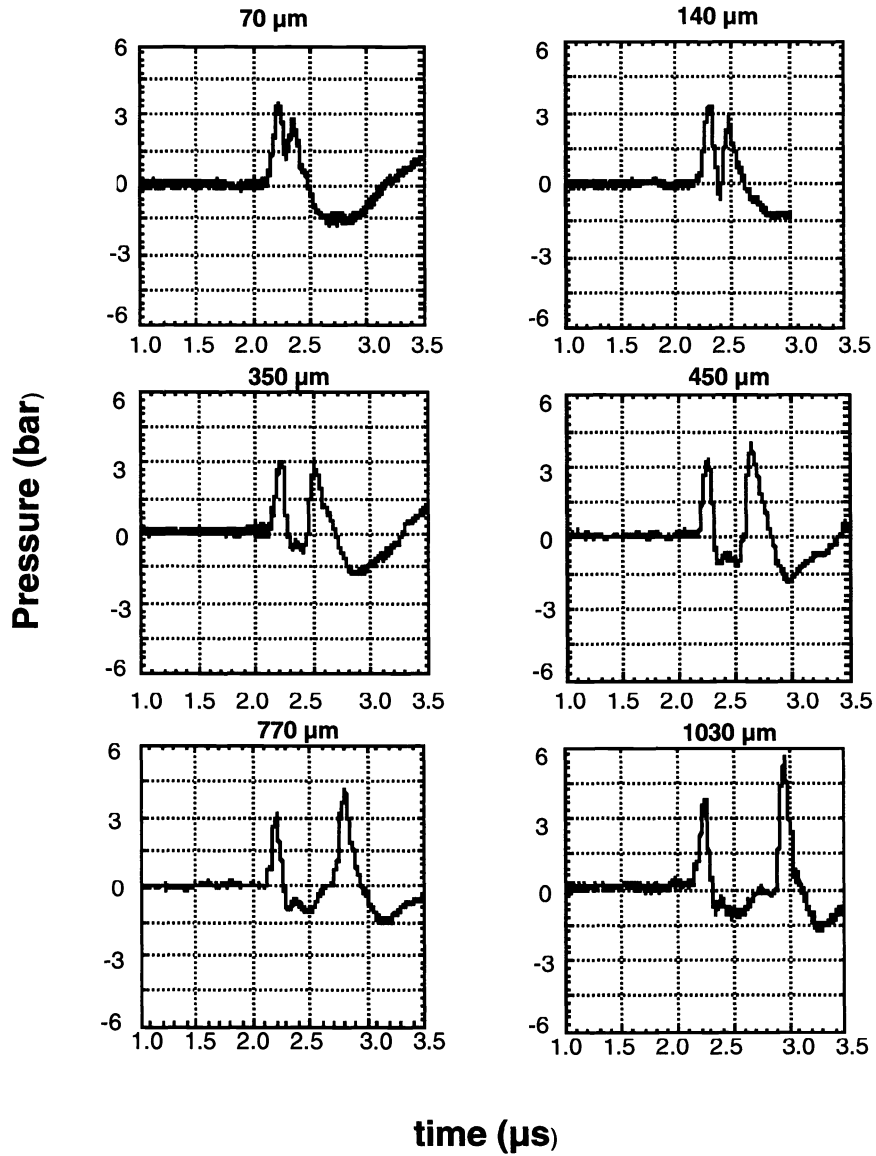


Figure 4. The separations of the epidermal and PWS peaks are shown here. The PWS peak decreases in amplitude as it merges with the negative diffractive signal from the epidermal signal.

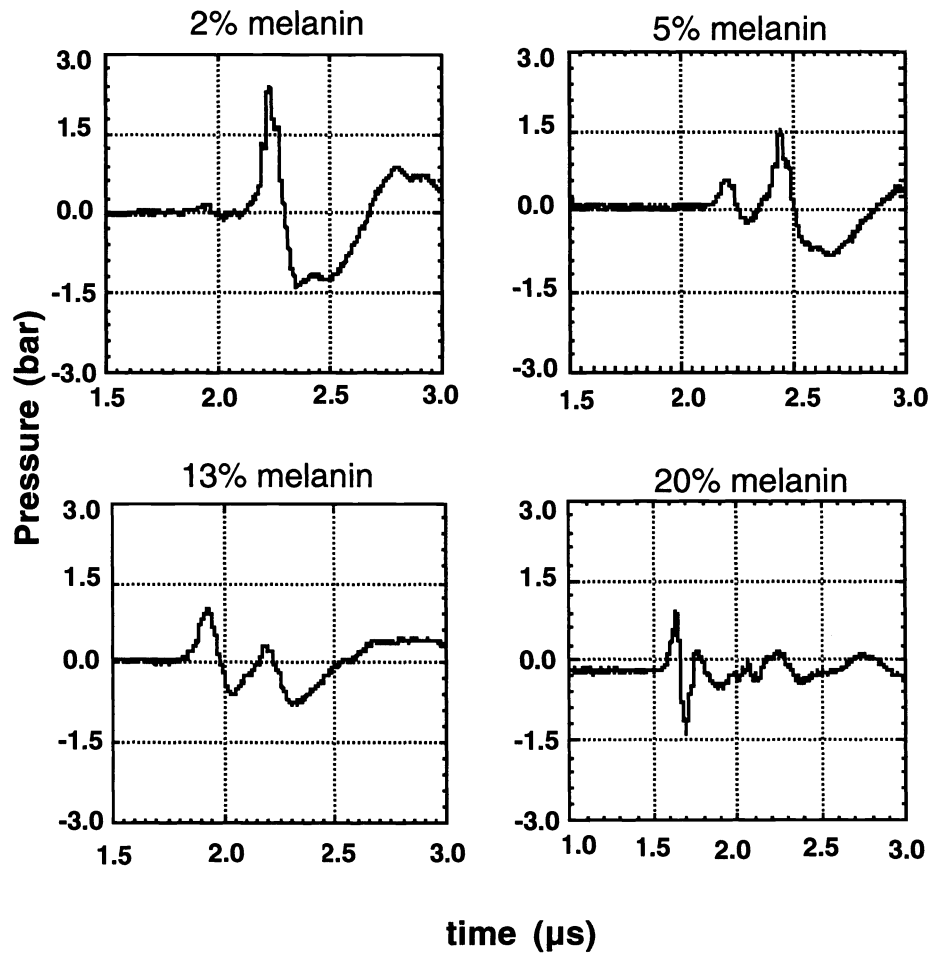


Figure 5. The epidermal melanin layers were modeled by absorbing superficial layers in the tissue phantoms. While PWS signals are evident for the 2, 5, and 13% melanin cases, at 20% the PWS is not seen at all.

3.2. Epidermal Melanin Content

A montage of the photoacoustic waves from the epidermal filtering experiments is shown in figure 5.

4. DISCUSSION

PWS depths have been studied using *in vivo* techniques, including pulsed photothermal radiometry (PPTR) [12, 13] and optical Doppler tomography (ODT) [14, 15]. PPTR requires the use of inversion algorithms to determine the initial light distribution after pulsed laser irradiation of PWS skin. The initial absorption is assumed to correspond to the structures within skin, including epidermal melanin and hemoglobin within the PWS lesion. Optimization of the inverse algorithms is problematic and accurate depth determination is difficult beyond $500\ \mu\text{m}$ [12]. In addition, calculation of temperature is sensitive to computational parameters, making absolute determination of temperature difficult. Using ODT, blood flow is used to determine the depth of the PWS lesions. Since there is no flow associated with melanin, the optical absorption in the epidermis is

not determined with this method. Also, due to the high optical scattering in skin, ODT signals are weak or nonexistent at depths greater than $500\ \mu\text{m}$ [7].

In this paper we have shown that the photoacoustic probe can discriminate epidermal melanin layers and PWS and can be used in patients with at least 13% epidermal melanin. Perhaps most importantly, the photoacoustic signals represent *the exact initial temperature distribution in skin*, corresponding to epidermal melanin and PWS vessels. The structure of PWS skin is shown unambiguously by the photoacoustic waveforms, allowing the clinician to optimize laser and CSC treatment parameters.

4.1. Layer Discrimination

The photoacoustic probe was able to discriminate two absorbing layers at all separation distances, including the $70\ \mu\text{m}$ layer. While such a non-turbid phantom doesn't account for optical scattering in skin, we wished to determine the minimum separation distance under ideal conditions. The thinnest clear layer we could make was $70\ \mu\text{m}$, though the photoacoustic waveform indicates that the signals between the two absorbing layers may have retained distinct peaks with as little as $50\ \mu\text{m}$ distance or less. Factors that would increase the distance at which the two layers can be discriminated include geometric diffraction of the acoustic waves and attenuation of the PWS signal. Thus, increased light scattering or decreased hemoglobin content in the PWS may affect the result. Also, a departure from a simple planar geometry of PWS lesions would increase acoustic diffraction and make discrimination more difficult.

At $1030\ \mu\text{m}$, the peaks are resolved enough that diffraction is evident in the waveform, indicated by the negative dip after the epidermal peak. As the PWS peak becomes more shallow, this diffraction will partially negate the PWS signal. The evolution of the sinking PWS amplitude is evident in the montage, so that once the separation is only $70\ \mu\text{m}$, the PWS peak is actually lower than the epidermal peak. Thus, for shallow PWS, it may be more difficult to detect a photoacoustic signal, particularly for weakly absorbing lesions.

4.2. Maximum Melanin Content for Threshold Detection of PWS

The experiments for threshold detection of PWS showed that with an optical depth of 0.34, a photoacoustic signal from the PWS could be detected. This corresponded to a 13% epidermal melanin volume fraction, or skin type III. Threshold detection is dependent on other factors, though, including epidermis to PWS separation and PWS absorption. We used a $250\ \mu\text{m}$ separation, which is reasonable for most lesions. Also, a PWS absorption coefficient of $25\ \text{cm}^{-1}$ represents a blood volume fraction of about 10%, which is a typical value. Thus, threshold detection should be scaled by PWS color and depth, though epidermal melanin content is the dominant factor.

4.3. Use of Acrylamide Phantoms for PWS Skin

The acrylamide phantoms were used to simulate human tissue, including epidermis, healthy dermis, and PWS lesion. While the layer discrimination experiments neglected optical scattering, experiments regarding maximum melanin content were designed to emulate optical and acoustic properties of skin, *in vivo*. In fact, comparison of the photoacoustic signal from the 5% melanin layer and the signal from irradiation of a PWS in human patient with skin type I-II show remarkable similarity (figure 6). The human skin would probably have an epidermal melanin volume fraction of 3-4%, thus the slight increase in the relative amplitude of the epidermal signal in the 5% phantom. Otherwise, the signals from the phantom and the human patient are almost indistinguishable.

5. CONCLUSIONS

The photoacoustic probe described in this paper can discriminate between absorbing layers in ideal tissue phantoms that are separated by as little as $70\ \mu\text{m}$ of a non-absorbing layer. For actual tissue, with light scattering and non-planar layers, the necessary separation will be greater. Using a turbid phantom that approximated human skin, the probe was able to detect a PWS layer with an epidermal melanin layer with an absorption coefficient of $52\ \text{cm}^{-1}$ and a thickness of $75\ \mu\text{m}$, for a total optical density of 0.34. Detection may be more favorable for more highly absorbing PWS. Finally, the acrylamide phantoms were shown to generate photoacoustic waves closely resembling those generated by human PWS, *in vivo*.

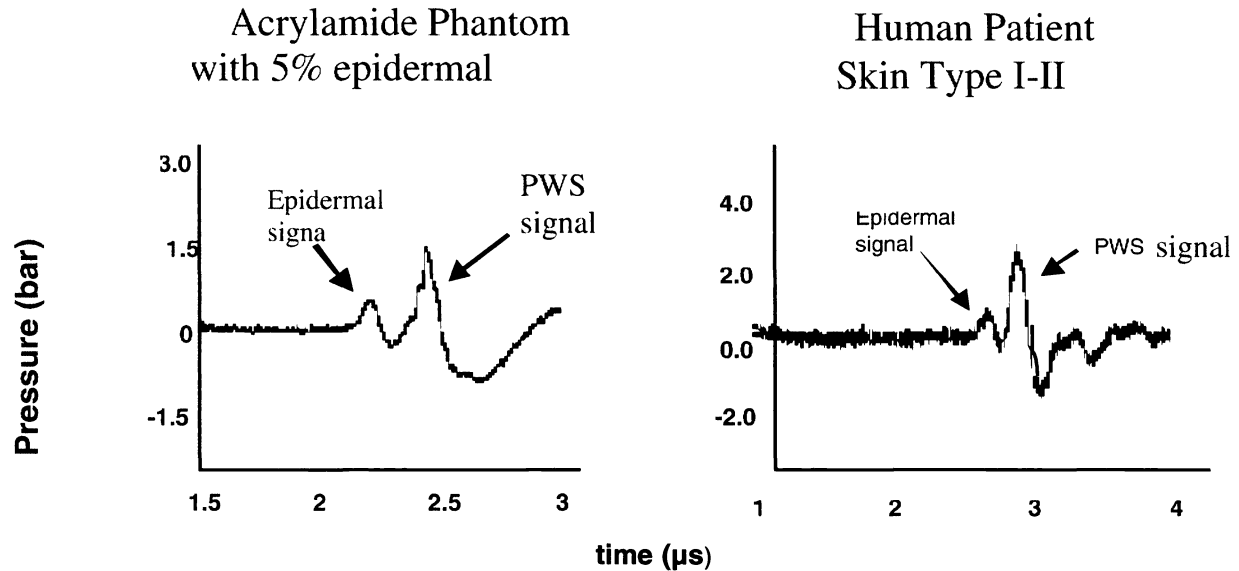


Figure 6. The photoacoustic signals from the turbid acrylamide phantom with 5% epidermal melanin content and of human skin with PWS. Although the depths and pressures are different, the signals are similar in the epidermal and PWS profiles.

ACKNOWLEDGMENTS

We acknowledge the helpful advice of G. Paltauf, Z. Wang, G. Aguilar, and S. Jacques on probe design and implementation. This work was supported by research grants from the National Institutes of Health (AR43419, RR-01192) and U.S. Air Force Office of Scientific Research (F49620-00-1-0371).

REFERENCES

1. G. Aguilar, B. Majaron, J. A. Viator, B. Basinger, E. Karapetian, L. O. Svaasand, E. J. Lavernia, and J. S. Nelson, "Influence of spraying distance and post-cooling on cryogen spray cooling for dermatologic laser surgery," *Proc. SPIE* **4244**, 2001.
2. W. Verkruysse, B. Majaron, B. S. Tanenbaum, and J. S. Nelson, "Optimal cryogen spray cooling parameters for pulsed laser treatment of port wine stains," *Lasers Surg. Med.* **27**, pp. 165–170, 2000.
3. J. S. Nelson, B. Majaron, and K. M. Kelly, "Active skin cooling in conjunction with laser dermatologic surgery," *Sem. Cut. Med. Surg.* **19**, pp. 253–266, 2000.
4. A. A. Oraevsky, S. L. Jacques, and F. K. Tittel, "Determination of tissue optical properties by piezoelectric detection of laser-induced stress waves," *Proc. SPIE* **1882**, pp. 86–101, 1993.
5. J. A. Viator, S. L. Jacques, and S. A. Prahl, "Depth profiling of absorbing soft materials using photoacoustic methods," *J. Select. Topics Quantum Electron.* **5**, pp. 989–996, 1999.
6. J. A. Viator, G. Paltauf, S. L. Jacques, and S. A. Prahl, "Design and testing of an endoscopic photoacoustic probe for determining treatment depth after photodynamic therapy of esophageal cancer," *Proc. SPIE* **4256**, 2001.
7. J. A. Viator, G. P. G. Au, S. L. Jacques, S. A. Prahl, H. Ren, Z. Chen, and J. S. Nelson, "Clinical testing of a photoacoustic probe for port wine stain depth determination," *Lasers Surg. Med.* (accepted).
8. G. Paltauf, H. Schmidt-Kloiber, and H. Guss, "Light distribution measurements in absorbing materials by optical detection of laser-induced stress waves," *Appl. Phys. Lett.* **69**, pp. 1526–1528, 1996.
9. M. J. C. van Gemert, A. J. Welch, J. W. Pickering, and O. T. Tan, *Optical-Thermal Response of Laser-Irradiated Tissue*, ch. Laser treatment of port wine stains. New York: Plenum Press, 1995.

10. S. T. Flock, S. L. Jacques, B. C. Wilson, W. M. Star, and M. J. C. van Gemert, "Optical properties of intralipid: A phantom medium for light propagation studies," *Lasers Surg. Med.* **12**, pp. 510–519, 1992.
11. H. J. van Staveren, C. J. M. Moes, J. van Marle, S. A. Prahl, and M. J. C. van Gemert, "Light scattering in intralipid-10% in the wavelength range of 400–1100 nm," *Appl. Optics* **30**, pp. 4507–4514, 1991.
12. U. S. Sathyam and S. A. Prahl, "Limitations in measurement of subsurface temperatures using pulsed photothermal radiometry," *J. Biomed. Optics* **2**, pp. 251–261, 1996.
13. S. L. Jacques, J. S. Nelson, W. H. Wright, and T. E. Milner, "Pulsed photothermal radiometry of port-wine-stain lesions," *Appl. Optics* **32**, pp. 2439–2446, 1993.
14. Z. Chen, Y. Zhao, S. M. Srinivas, J. S. Nelson, N. Prakash, and R. D. Frostig, "Optical Doppler tomography," *J. Select. Topics Quantum Electron.* **5**, pp. 1134–1142, 1999.
15. Y. Zhao, Z. Chen, C. Saxer, S. Xiang, J. F. de Boer, and J. S. Nelson, "Phase-resolved optical coherence tomography and optical Doppler tomography for imaging blood flow in human skin with fast scanning speed and high velocity sensitivity," *Optics Lett.* **25**, pp. 114–116, 2000.